

# Robust Stabilization of the Space Station

## Final Report

JOHNSON  
GRANT

IN-18-CR

115094  
p.33

Bong Wie

Arizona State University

9/30/91

N92-32244

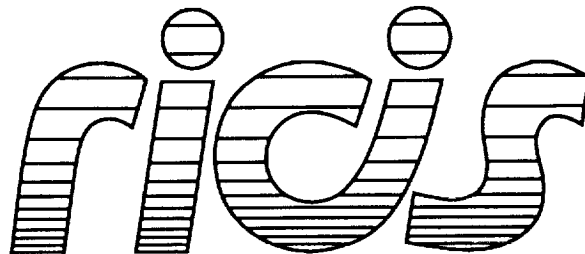
Unclas

G3/18 0115094

Cooperative Agreement NCC 9-16  
Research Activity No. MS.03

NASA Johnson Space Center  
Engineering Directorate  
Navigation Control and Aeronautics Division

(NASA-CR-190627) ROBUST  
STABILIZATION OF THE SPACE STATION  
Final Report (Research Inst. for  
Computing and Information Systems)  
33 p



Research Institute for Computing and Information Systems  
University of Houston-Clear Lake

## ***The RICIS Concept***

---

The University of Houston-Clear Lake established the Research Institute for Computing and Information Systems (RICIS) in 1986 to encourage the NASA Johnson Space Center (JSC) and local industry to actively support research in the computing and information sciences. As part of this endeavor, UHCL proposed a partnership with JSC to jointly define and manage an integrated program of research in advanced data processing technology needed for JSC's main missions, including administrative, engineering and science responsibilities. JSC agreed and entered into a continuing cooperative agreement with UHCL beginning in May 1986, to jointly plan and execute such research through RICIS. Additionally, under Cooperative Agreement NCC 9-16, computing and educational facilities are shared by the two institutions to conduct the research.

The UHCL/RICIS mission is to conduct, coordinate, and disseminate research and professional level education in computing and information systems to serve the needs of the government, industry, community and academia. RICIS combines resources of UHCL and its gateway affiliates to research and develop materials, prototypes and publications on topics of mutual interest to its sponsors and researchers. Within UHCL, the mission is being implemented through interdisciplinary involvement of faculty and students from each of the four schools: Business and Public Administration, Education, Human Sciences and Humanities, and Natural and Applied Sciences. RICIS also collaborates with industry in a companion program. This program is focused on serving the research and advanced development needs of industry.

Moreover, UHCL established relationships with other universities and research organizations, having common research interests, to provide additional sources of expertise to conduct needed research. For example, UHCL has entered into a special partnership with Texas A&M University to help oversee RICIS research and education programs, while other research organizations are involved via the "gateway" concept.

A major role of RICIS then is to find the best match of sponsors, researchers and research objectives to advance knowledge in the computing and information sciences. RICIS, working jointly with its sponsors, advises on research needs, recommends principals for conducting the research, provides technical and administrative support to coordinate the research and integrates technical results into the goals of UHCL, NASA/JSC and industry.

***Robust Stabilization  
of the Space Station***

***Final Report***

THE UNIVERSITY OF CHICAGO

1964

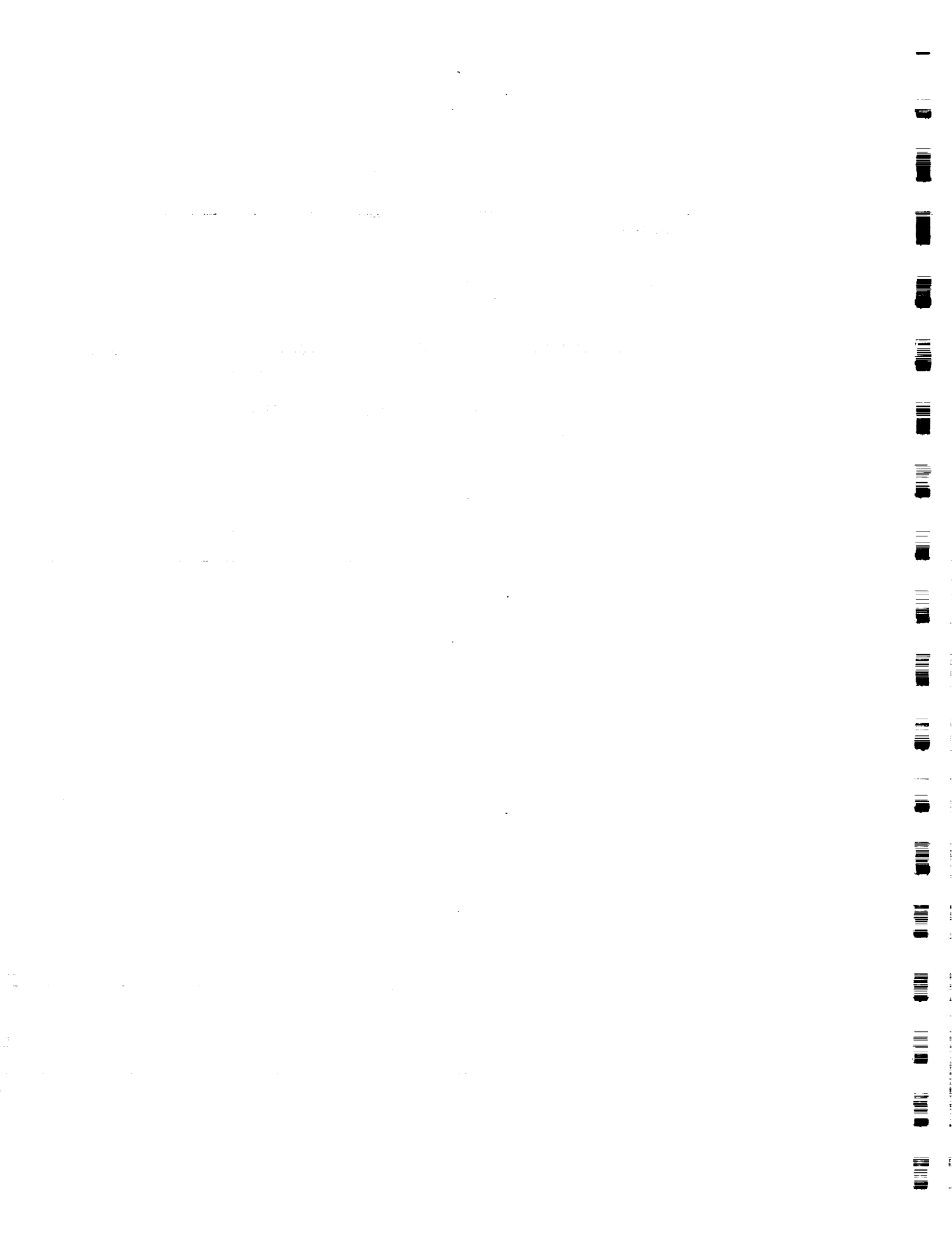


## **RICIS Preface**

This research was conducted under auspices of the Research Institute for Computing and Information Systems. Dr. Bong Wie of Arizona State University acted as Principal Investigator. Dr. Glen Houston served as RICIS research coordinator.

Funding was initially provided by the Mission Planning and Analysis Division, NASA/JSC through Cooperative Agreement NCC 9-16 between the NASA Johnson Space Center and the University of Houston-Clear Lake; funding was later provided by the Navigation Control and Aeronautics Division, Engineering Directorate after a NASA reorganization. The initial NASA research coordinator for this activity was David K. Geller; later John W. Sunkel of the Navigation Control and Aeronautics Division, Engineering Directorate, NASA/JSC assumed that role.

The views and conclusions contained in this report are those of the authors and should not be interpreted as representative of the official policies, either express or implied, of UHCL, RICIS, NASA or the United States Government.



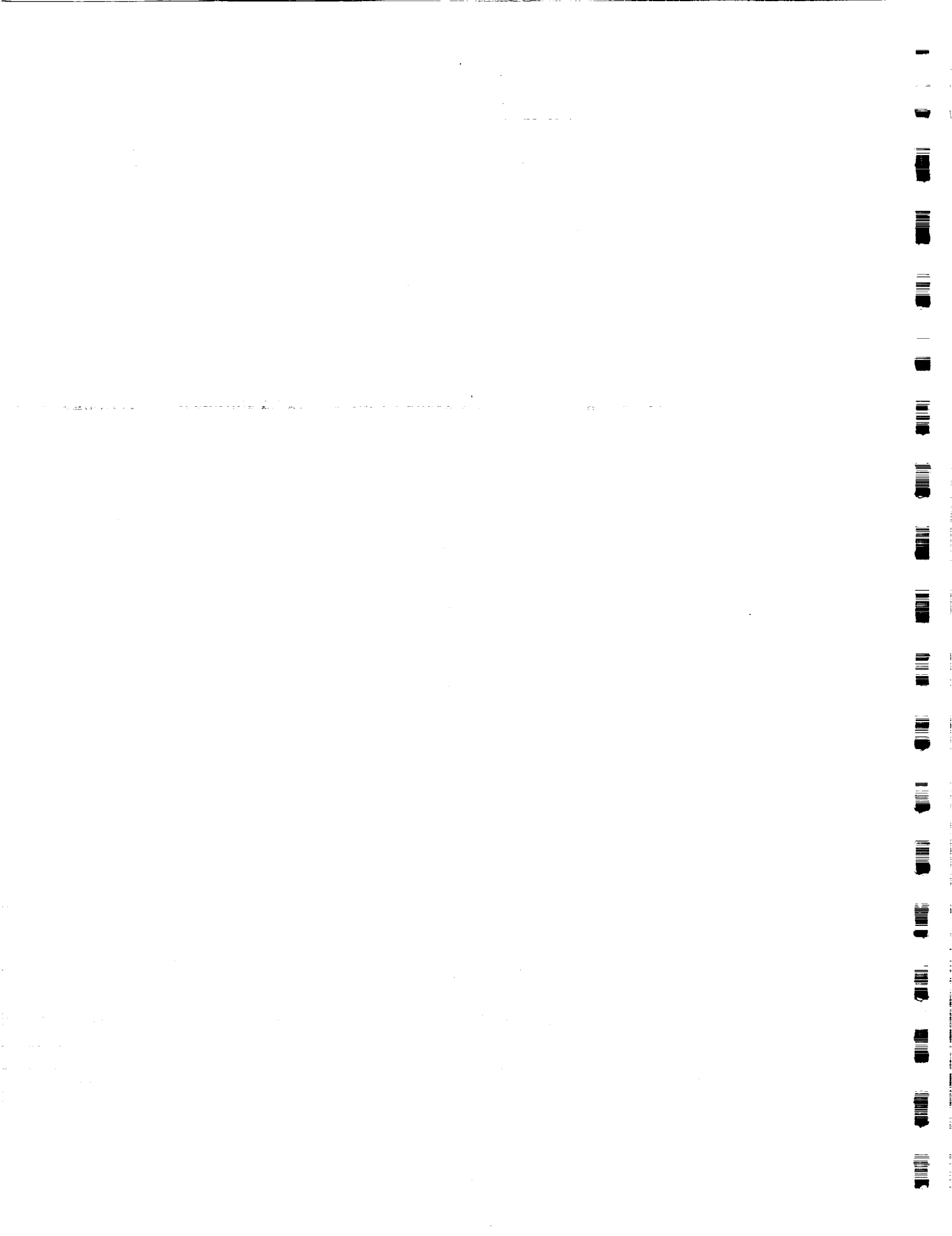
## RICIS Table of Contents

### Part One:

*Interim Progress Report, June 7, 1991*

### Part Two:

*Robust  $H_\infty$  Control Design for the Space Station with Structured Parameter Uncertainty*



# Arizona State University

---

College of Engineering and Applied Sciences  
Department of Mechanical and Aerospace Engineering  
Tempe, Arizona 85287-6106  
602/965-3291  
FAX: 602/965-1384  
TLX 165878 COLL ENG TMPE

June 7, 1991

Lin Reece, Contracts Manager  
Office of Sponsored Programs  
Box 44  
University of Houston - Clear Lake  
2700 Bay Area Blvd  
Houston, TX 77058-1098

RE: Progress Report for RICIS Research Activity No. MS03  
(NASA Cooperative Agreement NCC 9-16, ASU XAJ 6171)

Dear Ms. Reece:

This is to inform you that we have been making progress to accomplish all research tasks of the above referenced subcontract by September 30, 1991. In response to the request of Dr. John Sunkel, Technical Monitor at NASA JSC, we are going to complete this contract three months earlier than the extended expiration date of December 31, 1991.

We are currently preparing the final report for this contract, which will be delivered to you in September 1991.

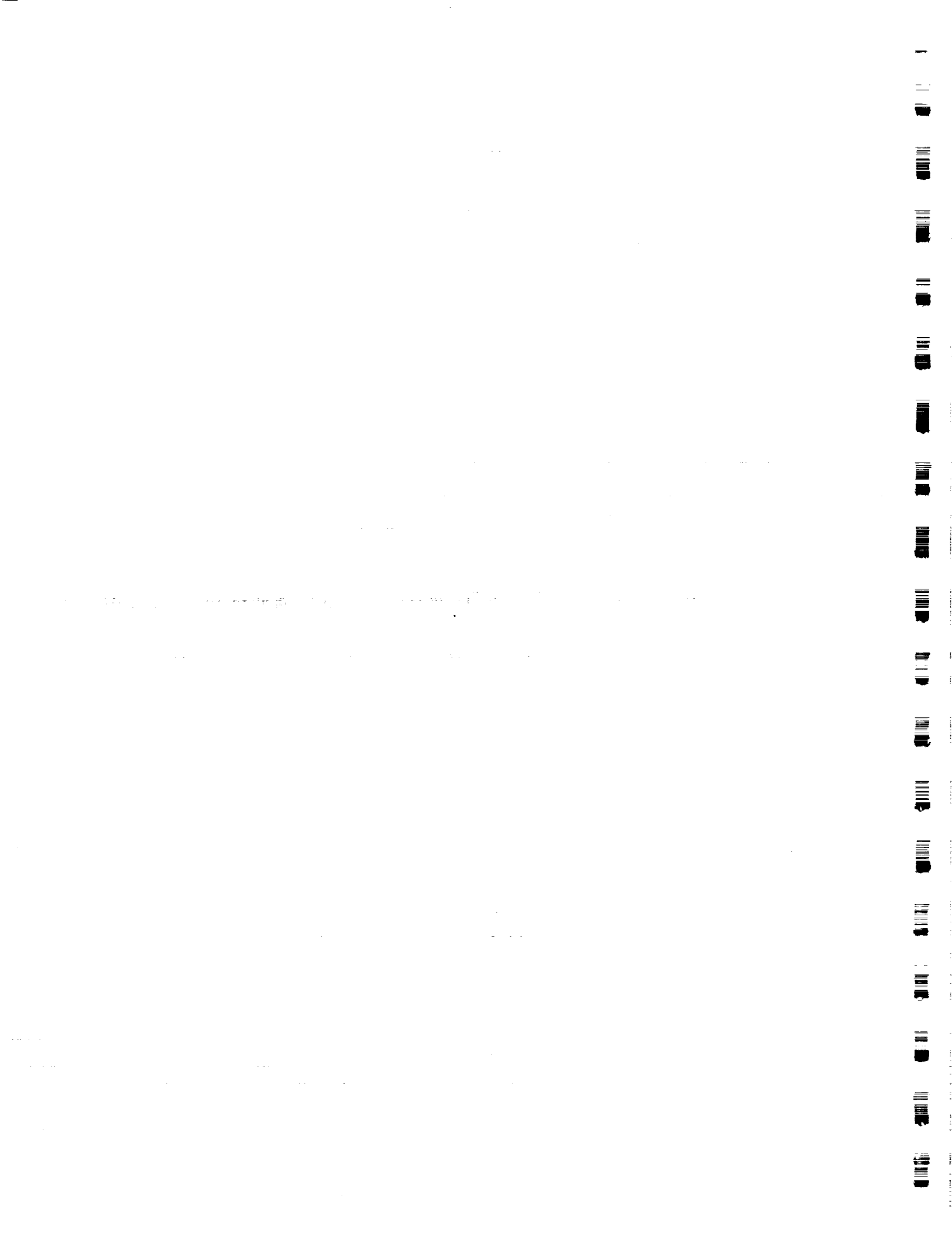
If you need additional information, please call me at (602) 965-8674 or 965-3291.

Sincerely,



Bong Wie  
Principal Investigator

cc: Dottie Sparks  
ASU Office of Sponsored Projects



**Final Report**

**RICIS MS 03**

**Robust Stabilization of the Space Station**

**by**

**Bong Wie**

**Dept. of Mechanical & Aerospace Engineering  
Arizona State University  
Tempe, AZ 85287-6106**

**Prepared for**

**RICIS  
University of Houston - Clear Lake  
Houston, Texas 77058-1098**

**September 30, 1991**



# **Robust Stabilization of the Space Station**

**Final Report**  
**September 30, 1991**

**Grant Number:** RICIS Research Activity No. MS 03

**Period of Work:** October 1, 1990 - September 30, 1991

**Principal Investigator:** Dr. Bong Wie  
Dept. of Mechanical & Aerospace Engineering  
Arizona State University  
Tempe, AZ 85287-6106  
(602) 965-8674

**Submitted to:** Dr. Glen Houston, Director  
RICIS  
University of Houston - Clear Lake  
2700 Bay Area Blvd  
Houston, Texas 77058-1098



# Robust $H_\infty$ Control Design for the Space Station with Structured Parameter Uncertainty

Kuk-Whan Byun\* and Bong Wie†  
Arizona State University  
Tempe, Arizona

David Geller‡ and John Sunkel§  
NASA Johnson Space Center  
Houston, Texas

## Abstract

A robust  $H_\infty$  control design methodology and its application to a Space Station attitude and momentum control problem are presented. This new approach incorporates nonlinear multi-parameter variations in the state-space formulation of  $H_\infty$  control theory. An application of this robust  $H_\infty$  control synthesis technique to the Space Station control problem yields a remarkable result in stability robustness with respect to the moments-of-inertia variation of about 73% in one of the structured uncertainty directions. The performance and stability of this new robust  $H_\infty$  controller for the Space Station are compared to those of other controllers designed using a standard linear-quadratic-regulator synthesis technique.

---

\*Currently, Research Scientist at Dynacs Engineering Co., Inc., Clearwater, Florida.

†Associate Professor, Dept. of Mechanical and Aerospace Engineering, Associate Fellow AIAA.

‡Aerospace Engineer, Mission Planning and Analysis Division, Member AIAA.

§Aerospace Engineer, Avionics Division, Member AIAA.

## 1. Introduction

The Space Station Freedom will employ control moment gyros (CMGs) as primary actuating devices during normal flight mode operation, and it will utilize the gravity-gradient torque for the CMG momentum management [1,2]. An attitude determination system of the Space Station will employ rate gyros and star trackers to compute the states of the vehicle for control purposes. Multivariable, periodic-disturbance accommodating controllers have been developed and are being considered for actual implementation to the Space Station Freedom [3-7].

As illustrated in Fig. 1, the Space Station will be assembled and maintained using the Mobile Remote Manipulator System (MRMS) and its Mobile Transporter (MT). The MRMS/MT carrying a large payload will cause significant changes in the inertia property of the Space Station; consequently, it will affect the overall performance and stability of the control system. Study results on the effects of such MRMS/MT operations (e.g., a "bay" translation along the pitch axis and 180-deg slew maneuver about the pitch axis) can be found in [7]. The study results of [7] indicate that some form of adaptive or robust control with more than 50% inertia variation margins is necessary to account for the large changes in the inertia property caused by the motion of the MRMS/MT and its large payload. The study results also indicate that a high-bandwidth controller has unacceptable transient responses during the payload maneuvers.

In this paper, a robust control synthesis technique based on  $H_\infty$  control theory is developed and applied to the robust control design problem of the Space Station discussed above. This new approach incorporates nonlinear multi-parameter variations in the state-space formulation of  $H_\infty$  control theory [8-10]. An application of this robust  $H_\infty$  control synthesis technique to the Space Station yields a remarkable result in stability robustness with respect to the moments-of-inertia variation of about 73% in one of the structured uncertainty directions. Such a 73% inertia variation margin is rather significant compared to the margin of 44% of a typical linear-quadratic-regulator (LQR) design [3-7] with nearly the same control bandwidth as the robust  $H_\infty$  controller.

This paper is organized as follows. In Section 2 a robust full-state feedback control synthesis technique based on the  $H_\infty$  control theory is presented, which exploits the concept of input-output decomposition of the uncertain system parameters [10-13]. A "full-state" feedback control is considered since the full states of the vehicle are available from an attitude determination system of the Space Station. A similar approach for the

dynamic compensator design can be found in [13]. The linearized equations of motion of the Space Station are reviewed in Section 3. A robust  $H_\infty$  controller is synthesized in Section 4, with special emphasis on the input-output decomposition of nonlinear, uncertain multi-parameters of the system.

## 2. Robust $H_\infty$ Control Synthesis

### Background

In recent years there has been a growing interest in robust stabilization and control based on  $H_\infty$  control theory [8-10,13-15], and substantial contributions have already been made to the state-space characterization of the  $H_\infty$  control problems [8,9]. Most standard  $H_\infty$ -related control techniques are, however, concerned with the sensitivity minimization with respect to the external disturbances, and are not directly related to the structured parameter uncertainty. Recently, a new way of incorporating parameter uncertainty in the robust  $H_\infty$  compensator design is developed in [10,13] by converting the parameter-insensitive control problem into a conventional  $H_\infty$  problem. The state-space solution to a standard  $H_\infty$  control problem in [8,9] is then utilized by redefining the structured parameter variations in terms of a fictitious input and output.

In this section, such a robust  $H_\infty$  control synthesis technique developed in [10,13] is reviewed with special emphasis on the new concept of "directional" parameterization of nonlinear, uncertain parameters. Only the "full-state" feedback control case is considered here since the Space Station control problem does not need the consideration of state estimation. A more general case with dynamic compensation can be found in [10,13].

The  $H_\infty$  space consists of functions which are bounded and stable. The  $H_\infty$ -norm of a real-rational matrix  $\mathbf{T}(s)$  is defined as

$$\begin{aligned}\|\mathbf{T}\|_\infty &\triangleq \sup\{\|\mathbf{T}(s)\| : \operatorname{Re}(s) > 0\} \\ &= \sup_\omega \|\mathbf{T}(j\omega)\| \\ &= \sup_\omega \bar{\sigma}[\mathbf{T}(j\omega)]\end{aligned}$$

where  $\bar{\sigma}[\mathbf{T}(j\omega)]$  denotes the largest singular value of  $\mathbf{T}(j\omega)$  for a given  $\omega$ .

In this paper, we consider a linear, time-invariant multivariable system described by [8,9]

$$\dot{\mathbf{x}}(t) = \mathbf{A} \mathbf{x}(t) + \mathbf{B}_1 \mathbf{w}(t) + \mathbf{B}_2 \mathbf{u}(t) \quad (1a)$$

$$\mathbf{z}(t) = \mathbf{C}_1 \mathbf{x}(t) + \mathbf{D}_{11} \mathbf{w}(t) + \mathbf{D}_{12} \mathbf{u}(t) \quad (1b)$$

where  $\mathbf{x}(t)$  is an  $n$ -dimensional state vector and is assumed to be directly measured,  $\mathbf{w}(t)$  an  $m_1$ -dimensional disturbance vector,  $\mathbf{u}(t)$  an  $m_2$ -dimensional control vector, and  $\mathbf{z}(t)$  a  $p_1$ -dimensional controlled output vector.

The transfer function representation of this system is given by

$$\mathbf{z}(s) = \begin{bmatrix} \mathbf{P}_{11}(s) & \mathbf{P}_{12}(s) \end{bmatrix} \begin{bmatrix} \mathbf{w}(s) \\ \mathbf{u}(s) \end{bmatrix} \quad (2)$$

while the plant transfer matrix  $\mathbf{P}(s)$  is related to the matrices in Eqs. (1) by

$$\mathbf{P}(s) = \mathbf{C}_1 (s\mathbf{I} - \mathbf{A})^{-1} \begin{bmatrix} \mathbf{B}_1 & \mathbf{B}_2 \end{bmatrix} + \begin{bmatrix} \mathbf{D}_{11} & \mathbf{D}_{12} \end{bmatrix} \quad (3)$$

### Internal Feedback Loop

Consider an uncertain dynamical system described as

$$\begin{bmatrix} \dot{\mathbf{x}} \\ \mathbf{z} \end{bmatrix} = \begin{bmatrix} \hat{\mathbf{A}} & \hat{\mathbf{B}}_1 & \hat{\mathbf{B}}_2 \\ \mathbf{C}_1 & \mathbf{D}_{11} & \mathbf{D}_{12} \end{bmatrix} \begin{bmatrix} \mathbf{x} \\ \mathbf{w} \\ \mathbf{u} \end{bmatrix} \quad (4)$$

where  $\mathbf{C}_1$ ,  $\mathbf{D}_{11}$ , and  $\mathbf{D}_{12}$  are not subject to parameter variations. The system matrices possessing uncertain parameters in Eq. (4) are linearly decomposed into an internal feedback loop [11,12,13] as follows:

$$\begin{bmatrix} \dot{\mathbf{x}} \\ \mathbf{z} \end{bmatrix} = \left\{ \begin{bmatrix} \mathbf{A} & \mathbf{B}_1 & \mathbf{B}_2 \\ \mathbf{C}_1 & \mathbf{D}_{11} & \mathbf{D}_{12} \end{bmatrix} + \Delta_e \right\} \begin{bmatrix} \mathbf{x} \\ \mathbf{w} \\ \mathbf{u} \end{bmatrix} \quad (5)$$

where the first matrix in the right-hand side is the nominal system matrix and  $\Delta_e$  is the perturbation matrix defined as

$$\Delta_e \triangleq \begin{bmatrix} \Delta \mathbf{A} & \Delta \mathbf{B}_1 & \Delta \mathbf{B}_2 \\ \mathbf{0} & \mathbf{0} & \mathbf{0} \end{bmatrix} \quad (6)$$

Suppose that there are  $l$  independent parameters  $p_1, \dots, p_l$  and that their variations are bounded as  $\underline{p}_i \leq p_i \leq \bar{p}_i$ , or  $|\Delta p_i| \leq 1$ . If  $\Delta_e$  is linearly dependent of each uncertain

parameter, then it can be decomposed as derived in [11,13]. However,  $\Delta_e$  may contain elements that are nonlinear combinations of  $\Delta p_i$ 's. Variations in the uncertain matrix elements,  $\Delta e_i$ , are represented in a functional form as

$$\Delta e_i = \Delta e_i(\Delta p) \quad \text{for } i = 1, \dots, q$$

where  $\Delta p = [\Delta p_1, \dots, \Delta p_l]^T$  and  $q$  is the number of the uncertain matrix elements of  $\Delta_e$ . The perturbation matrix  $\Delta_e$  is then decomposed as

$$\Delta_e = - \begin{bmatrix} M_x \\ 0 \end{bmatrix} E \begin{bmatrix} N_x & N_w & N_u \end{bmatrix} = -MEN \quad (7)$$

where the columns of  $M$  and the rows of  $N$  span the columns and the rows of  $\Delta_e$ , respectively; and

$$E = \begin{bmatrix} \Delta e_1(\Delta p) & & 0 \\ & \ddots & \\ 0 & & \Delta e_q(\Delta p) \end{bmatrix}. \quad (8)$$

If  $\Delta e_i$ 's are linear in  $\Delta p_i$ 's, then the above input-output decomposition can be rearranged to become a rank-one input-output decomposition, which has been applied to a real-parameter variation problem [13].

Define the following new variables

$$z_p \triangleq \begin{bmatrix} N_x & 0 & N_w & N_u \end{bmatrix} \begin{bmatrix} x \\ w_p \\ w \\ u \end{bmatrix}, \quad (9a)$$

$$w_p \triangleq -E z_p, \quad (9b)$$

then the perturbed system, Eq. (5), and the input-output decomposition, Eq. (7), can be combined as:

$$\begin{bmatrix} \dot{x} \\ z_p \\ z \end{bmatrix} = \begin{bmatrix} A & M_x & B_1 & B_2 \\ N_x & 0 & N_w & N_u \\ C_1 & 0 & D_{11} & D_{12} \end{bmatrix} \begin{bmatrix} x \\ w_p \\ w \\ u \end{bmatrix} \quad (10a)$$

$$w_p = -E z_p \quad (10b)$$

where  $w_p$  and  $z_p$  are considered as the fictitious input and output, respectively, caused by the plant perturbation; and  $E$  is considered as a fictitious, internal feedback loop gain matrix.

The above internal feedback loop representation of the plant parameter uncertainty becomes useful for stability/performance robustness analysis discussed later in this section. In fact, the parameter-insensitive control synthesis problem becomes a conventional  $H_\infty$  disturbance attenuation problem, which can be easily solved by using the state-space formulation of the  $H_\infty$  control theory.

### Directional Parameter Variations

A "hypercube" in the space of the plant parameters, centered at a nominal point, is often used as a stability robustness measure [16]. The robust control synthesis problem is then to find a controller which yields the largest hypercube that will fit within the existing, but unknown, region of stability in the plant's parameter space. In [16], a computational method is developed, which exploits the mapping theorem and the "multi-linear" property of the plant's uncertain parameters. However, as shown later in this paper, the Space Station has the uncertain moments of inertia which appear in the internal feedback loop gain  $E$  as nonlinear functions.

One way to overcome the presence of such uncertain parameters in the internal feedback loop modeling is to consider  $e_1, \dots, e_q$  of  $E$  as new independent parameters and to find the worst possible bounds  $e_i$  and  $\bar{e}_i$  for each  $e_i$ ; that is,  $e_i \leq e_i \leq \bar{e}_i$ . This approach then reduces to the standard input-output decomposition problem with  $q$  independent parameters. However,  $e_i$ 's may be functionally dependent to each other through actual parameter variations,  $\Delta p_i$ 's. Whenever  $e_i$ 's are closely related, this approach will result in a very conservative control design; furthermore, some valuable information on the structured parameter variations is not utilized in this approach.

In order to exploit some structured or directional information on the plant parameter variations, the internal feedback loop gain matrix  $E$  is linearized about the nominal parameter set with respect to small  $\Delta p_i$ 's as follows:

$$E \cong M_1 E_1 N_1 \quad (11a)$$

$$\Delta_e \cong -M M_1 E_1 N_1 N \quad (11b)$$

where  $E_1$  contains only the actual, independent uncertain parameters. The standard form of an input-output decomposition such as Eq. (7), is obtained by re-defining  $M$ ,

$N$ , and  $E$  as

$$\begin{aligned} M &\leftarrow M M_1 \\ N &\leftarrow N_1 N \\ E &\leftarrow E_1 \end{aligned} \quad (12)$$

In some cases, the plant parameter perturbations  $\Delta p_i$ 's may possess a certain *directional* relationship with the following form:

$$\Delta p_i = g_i \delta \quad \text{for } i = 1, \dots, l \quad (13)$$

where  $g_i$  represents the direction and magnitude of  $\Delta p_i$  and  $\delta$  is a scalar variable which represents the system uncertainty. Parameter variations involving a single parameter variable are referred to as *uni-directional* parameter variations, while those involving more than one parameter variable are referred to as *multi-directional* parameter variations.

The multi-directional parameter variations are characterized as:

$$\Delta p_i = g_{ij} \delta_j \quad \text{for } i = 1, \dots, l \text{ and } j = 1, \dots, r \quad (14)$$

where  $g_{ij}$  represents the direction and magnitude of  $\Delta p_i$  caused by  $\delta_j$  for multi-directional perturbations, and  $r$  is the number of independent uncertain parameters.

For such cases with multi-directional parameter variations, the internal feedback loop gain  $E$  in Eq. (8) becomes a function of  $\delta_j$ 's:

$$E = \begin{bmatrix} \Delta e_1(\delta) & & 0 \\ & \ddots & \\ 0 & & \Delta e_q(\delta) \end{bmatrix} \quad (15)$$

where  $\delta = [\delta_1, \dots, \delta_r]^T$ . Since  $E$  is nonlinear in  $\delta_j$ 's in general, the linearized input-output decomposition can be applied here, as in Eqs. (11) and (12), to be incorporated in the robust control synthesis.

### Stability/Performance Robustness

A robust  $H_\infty$  full-state feedback control synthesis technique presented in this section exploits the internal feedback loop modeling concept and the  $H_\infty$  control theory. This new robust control design methodology is summarized in terms of three theorems. Detailed proofs of these theorems can be found in [8-10]. Development and application of robust  $H_\infty$  compensator synthesis can be found in [13].

The parameter uncertainty model given by Eq. (7) and the nominal plant described by Eq. (2) can be combined as

$$\begin{bmatrix} z_p \\ z \\ x \end{bmatrix} = \begin{bmatrix} G_{11} & G_{12} & G_{13} \\ G_{21} & G_{22} & G_{23} \\ G_{31} & G_{32} & G_{33} \end{bmatrix} \begin{bmatrix} w_p \\ w \\ u \end{bmatrix} \quad (16a)$$

$$w_p = -Ez_p \quad (16b)$$

$$u = -Kx \quad (16c)$$

where  $w_p$  and  $z_p$  are, respectively, the fictitious input and output,  $E$  is the fictitious internal loop gain matrix, and  $K$  is a full-state gain matrix to be determined.

The closed-loop system, but with the fictitious internal loop open, becomes:

$$\begin{bmatrix} z_p \\ z \end{bmatrix} = T \begin{bmatrix} w_p \\ w \end{bmatrix} \quad (17a)$$

$$w_p = -Ez_p \quad (17b)$$

where

$$T = \begin{bmatrix} T_{11} & T_{12} \\ T_{21} & T_{22} \end{bmatrix} \quad (18a)$$

$$T_{11} = G_{11} - G_{13}K(I + G_{33}K)^{-1}G_{31} \quad (18b)$$

$$T_{12} = G_{12} - G_{13}K(I + G_{33}K)^{-1}G_{32} \quad (18c)$$

$$T_{21} = G_{21} - G_{23}K(I + G_{33}K)^{-1}G_{31} \quad (18d)$$

$$T_{22} = G_{22} - G_{23}K(I + G_{33}K)^{-1}G_{32} \quad (18e)$$

The actual closed-loop transfer function matrix from  $w$  to  $z$  with plant perturbations becomes

$$T_{zw} = T_{22} - T_{21}E(I + T_{11}E)^{-1}T_{12} \quad (19)$$

Note that, in Eqs. (16) and (17), the parameter uncertainty does not appear in the transfer function matrices. Equations (17) can be used for the stability/performance robustness characterization. Sufficient conditions for robust stability and performance are provided by the following Theorems 1 and 2.

#### Theorem 1 (Stability Robustness)

$T_{zw}(s, \alpha E) \forall \alpha \in [0,1]$  is robustly stable for  $\|E\| \leq \epsilon$ , and  $\epsilon > 0$ , if

$$\|T_{11}(s)\|_{\infty} < \epsilon^{-1}$$

where  $\epsilon$  is a measure of the magnitude of the plant parameter uncertainty  $E$  in Eq. (8).

It is seen that  $T_{11}$  determines the stability robustness with respect to parameter uncertainty. Small  $\|T_{11}\|_\infty$  allows large parameter variations for closed-loop stability. For this reason  $T_{11}$  is often referred to as robustness function [12]. The above theorem provides a sufficient condition for the closed-loop stability, resulting in a conservative control design. Since the condition in Theorem 1 is concerned with a deterministic bound, the  $H_\infty$  control theory can be employed for the internal feedback loop model. The next theorem provides a sufficient condition for guaranteed performance robustness.

**Theorem 2 (Performance Robustness)**

$T_{zw}(s, \alpha E) \forall \alpha \in [0,1]$  is stable, and  $\|T_{zw}(s, \alpha E)\|_\infty < \gamma \forall \alpha \in [0,1]$  with  $\|E\| \leq \gamma^{-1}$ , if

$$\|T\|_\infty < \gamma \quad (20)$$

where  $T$  and  $T_{zw}$  are defined in Eqs. (17) and (19), and  $\gamma$  is an upper bound for the desired performance specification.

The above two theorems provide conditions for robust stability and performance of the perturbed closed-loop system in terms of  $T_{11}$  and  $T$  in Eqs. (17) and (18). The following re-definition of  $z$ ,  $w$ , and the associated matrices enables us to employ the standard state-space representation given by Eq. (1):

$$\begin{aligned} z &\leftarrow \begin{bmatrix} z_p \\ z \end{bmatrix}, & w &\leftarrow \begin{bmatrix} w_p \\ w \end{bmatrix}, \\ B_1 &\leftarrow \begin{bmatrix} M_x & B_1 \end{bmatrix}, & C_1 &\leftarrow \begin{bmatrix} N_x \\ C_1 \end{bmatrix}, \\ D_{11} &\leftarrow \begin{bmatrix} 0 & N_w \\ 0 & D_{11} \end{bmatrix}, & D_{12} &\leftarrow \begin{bmatrix} N_u \\ D_{12} \end{bmatrix}. \end{aligned} \quad (21)$$

The following theorem [8] gives a robust  $H_\infty$  controller which satisfies the condition in Eq. (20).

**Theorem 3 ( $H_\infty$  Full-State Feedback Controller)** Assume that

- (i)  $(A, B_2)$  is stabilizable and  $(C_1, A)$  is detectable,
- (ii)  $D_{12}^T \begin{bmatrix} C_1 & D_{12} \end{bmatrix} = \begin{bmatrix} 0 & I \end{bmatrix}$ ,

(iii) the rank of  $P_{12}(j\omega)$  is  $m_2$  for all  $\omega$ , and

(iv)  $D_{11} = 0$ .

Given the above assumptions (i) through (iv), there exists an internally stabilizing controller such that, for the closed-loop transfer matrix  $T$  in Eqs. (17) and for a given design variable  $\gamma$ ,

$$\|T\|_{\infty} < \gamma$$

if and only if the following Riccati equations

$$0 = A^T X + X A - X(B_2 B_2^T - \frac{1}{\gamma^2} B_1 B_1^T) X + C_1^T C_1 \quad (22)$$

have unique symmetric positive semi-definite solution  $X$  such that

$$A - (B_2 B_2^T - \frac{1}{\gamma^2} B_1 B_1^T) X \text{ and } A - B_2 B_2^T X \text{ are stable.}$$

A state-feedback gain that satisfies  $\|T_{zw}\|_{\infty} < \gamma$ , where  $\gamma$  is a design variable specifying an upper bound of the perturbed closed-loop performance  $T_{zw}$ , is then obtained as

$$K = B_2^T X \quad (23)$$

In order to achieve the desired closed-loop performance over all frequencies,  $T_{zw}$  is often formulated to include frequency-dependent weighting matrices. (A proper selection of the weighting matrices is an important step in any optimization-based design techniques, such as the linear-quadratic-gaussian (LQG) control and  $H_{\infty}$ -optimization.) In this paper, constant diagonal weighting matrices are used. Inverses of the diagonal elements of the weighting matrix is referred to as weighting factors. The weighting factors and  $\gamma$  represent relative input-output levels and overall closed-loop performance level, respectively. In the Appendix, the usage of constant weightings, scaling, and orthogonal transformations on  $u$ ,  $w$ , and  $z$  for practical implementation of Theorem 3 are briefly summarized.

### 3. Space Station Model

The robust control synthesis technique developed in Section 2 is applied to the Space Station subject to large payload operations which cause significant changes in the moments of inertia of the system. Dynamical equations of the Space Station are briefly reviewed (for details, see [3,4]).

The Space Station in a circular orbit is expected to maintain local-vertical and local-horizontal (LVLH) orientation during normal mode operation. For small attitude deviations from LVLH orientation, the linearized equations of motion can be written as:

Space Station Dynamics:

$$\begin{aligned}
 & \begin{bmatrix} I_{11} & I_{12} & I_{13} \\ I_{21} & I_{22} & I_{23} \\ I_{31} & I_{32} & I_{33} \end{bmatrix} \begin{bmatrix} \dot{\omega}_1 \\ \dot{\omega}_2 \\ \dot{\omega}_3 \end{bmatrix} \\
 &= n \begin{bmatrix} I_{31}, & 2I_{32}, & I_{33} - I_{22} \\ -I_{32}, & 0, & I_{12} \\ I_{22} - I_{11}, & -2I_{12}, & -I_{13} \end{bmatrix} \begin{bmatrix} \omega_1 \\ \omega_2 \\ \omega_3 \end{bmatrix} \\
 &+ 3n^2 \begin{bmatrix} I_{33} - I_{22}, & I_{21}, & 0 \\ I_{12}, & I_{33} - I_{11}, & 0 \\ -I_{13}, & -I_{23}, & 0 \end{bmatrix} \begin{bmatrix} \theta_1 \\ \theta_2 \\ \theta_3 \end{bmatrix} \\
 &+ n^2 \begin{bmatrix} -2I_{23} \\ 3I_{13} \\ -I_{12} \end{bmatrix} + \begin{bmatrix} -u_1 + w_1 \\ -u_2 + w_2 \\ -u_3 + w_3 \end{bmatrix} \tag{24}
 \end{aligned}$$

Attitude Kinematics:

$$\dot{\theta}_1 - n\theta_3 = \omega_1 \tag{25a}$$

$$\dot{\theta}_2 - n = \omega_2 \tag{25b}$$

$$\dot{\theta}_3 + n\theta_1 = \omega_3 \tag{25c}$$

CMG Momentum:

$$\dot{h}_1 - nh_3 = u_1 \tag{26a}$$

$$\dot{h}_2 = u_2 \tag{26b}$$

$$\dot{h}_3 + nh_1 = u_3 \tag{26c}$$

where (1, 2, 3) are the roll, pitch, and yaw control axes whose origin is fixed at the mass center, with the roll axis in the flight direction, the pitch axis perpendicular to the orbit plane, and the yaw axis toward the Earth;  $(\theta_1, \theta_2, \theta_3)$  are the roll, pitch, yaw Euler angles of the body axes with respect to LVLH axes which rotate with the orbital angular velocity,  $n$ ;  $(\omega_1, \omega_2, \omega_3)$  are the body-axis components of the absolute angular velocity of the station;  $(I_{11}, I_{22}, I_{33})$  are the principal moments of inertia;  $I_{ij}$  ( $i \neq j$ ) are the products of inertia;  $(h_1, h_2, h_3)$  are the body-axis components of the CMG momentum;  $(u_1, u_2, u_3)$  are the body-axis components of the control torque caused by

CMG momentum change;  $(w_1, w_2, w_3)$  are the body-axis components of the external disturbance torque; and  $n$  is the orbital rate of 0.0011 rad/sec.

Note that the products of inertia cause three-axis coupling as well as a bias torque in each axis. Fortunately, most practical situations with small products of inertia permit further simplification in such a way that pitch motion is uncoupled from roll/yaw motion. For the case where the control axes are nearly aligned with the principal axes ( $I_1 \triangleq I_{11}$ ,  $I_2 \triangleq I_{22}$ , and  $I_3 \triangleq I_{33}$ ), Eqs. (24) become

$$\dot{\omega}_1 + nk_1\omega_3 + 3n^2k_1\theta_1 = -b_1u_1 + b_1w_1 \quad (27a)$$

$$\dot{\omega}_2 + 3n^2k_2\theta_2 = -b_2u_2 + b_2w_2 \quad (27b)$$

$$\dot{\omega}_3 - nk_3\omega_1 = -b_3u_3 + b_3w_3 \quad (27c)$$

where

$$\begin{aligned} k_1 &= (I_2 - I_3)/I_1, & b_1 &= 1/I_1, \\ k_2 &= (I_1 - I_3)/I_2, & b_2 &= 1/I_2, \\ k_3 &= (I_2 - I_1)/I_3, & b_3 &= 1/I_3. \end{aligned}$$

Inertia matrices of the Phase 1 Space Station as well as the assembly flight #3 are listed in Table 1. In this paper, only the Phase 1 configuration is considered. The uncontrolled Space Station with such inertia properties is in an unstable equilibrium when  $\theta_i = 0$  ( $i = 1, 2, 3$ ). Also included are expected aerodynamic disturbances which are modeled as bias plus cyclic terms in the body-fixed control axes:

$$w(t) = \text{Bias} + A_n \sin(nt + \phi_n) + A_{2n} \sin(2nt + \phi_{2n}) \quad (28)$$

The cyclic component at orbital rate is due to the effect of Earth's diurnal bulge, while the cyclic torque at twice the orbital rate is caused by the rotating solar panels. The magnitudes and phases of aerodynamic torque in each axis are unknown for control design.

#### 4. Space Station Control

A robust  $H_\infty$  control design for the Space Station is described here. The Space Station is desired to have a control system which accommodates the periodic disturbances and large inertia variations. In [3,4], a periodic-disturbance accommodating controller is developed for the Space Station, and the disturbance rejection filters for the control

of  $h_1, \theta_2, \theta_3$  are assumed to have the following forms:

$$\bar{\alpha}_1 + (n)^2 \alpha_1 = h_1 \quad (29a)$$

$$\bar{\beta}_1 + (2n)^2 \beta_1 = h_1 \quad (29b)$$

$$\bar{\alpha}_2 + (n)^2 \alpha_2 = \theta_2 \quad (29c)$$

$$\bar{\beta}_2 + (2n)^2 \beta_2 = \theta_2 \quad (29d)$$

$$\bar{\alpha}_3 + (n)^2 \alpha_3 = \theta_3 \quad (29e)$$

$$\bar{\beta}_3 + (2n)^2 \beta_3 = \theta_3 \quad (29f)$$

The pitch control logic, involving the single control input  $u_2$  and eight states, is then expressed as

$$u_2 = K_{22} \mathbf{x}_2 \quad (30)$$

where  $K_{22}$  is a  $1 \times 8$  gain matrix and  $\mathbf{x}_2$  is the state vector defined as

$$\mathbf{x}_2 \triangleq [\theta_2 \dot{\theta}_2 h_2 \int h_2 \alpha_2 \dot{\alpha}_2 \beta_2 \dot{\beta}_2]^T. \quad (31)$$

The CMG momentum and its integral are included to prevent CMG momentum build-up.

Similarly the roll/yaw control logic is given by two control inputs,  $u_1$  and  $u_3$ , and sixteen states:

$$\begin{bmatrix} u_1 \\ u_3 \end{bmatrix} = \begin{bmatrix} K_{11} & K_{13} \\ K_{31} & K_{33} \end{bmatrix} \begin{bmatrix} \mathbf{x}_1 \\ \mathbf{x}_3 \end{bmatrix} \quad (32)$$

where  $K_{ij}$ 's are  $1 \times 8$  gain matrices and

$$\mathbf{x}_1 \triangleq [\theta_1 \omega_1 h_1 \int h_1 \alpha_1 \dot{\alpha}_1 \beta_1 \dot{\beta}_1]^T, \quad (33a)$$

$$\mathbf{x}_3 \triangleq [\theta_3 \omega_3 h_3 \int h_3 \alpha_3 \dot{\alpha}_3 \beta_3 \dot{\beta}_3]^T. \quad (33b)$$

Directional inertia variations for the Space Station are modeled as

$$\begin{bmatrix} \Delta I_1 & \Delta I_2 & \Delta I_3 \end{bmatrix} = \delta_1 \begin{bmatrix} I_1 & 0 & I_1 \end{bmatrix} \quad (34a)$$

$$\begin{bmatrix} \Delta I_1 & \Delta I_2 & \Delta I_3 \end{bmatrix} = \delta_2 \begin{bmatrix} I_1 & I_2 & I_3 \end{bmatrix} \quad (34b)$$

$$\begin{bmatrix} \Delta I_1 & \Delta I_2 & \Delta I_3 \end{bmatrix} = \delta_3 \begin{bmatrix} I_1 & 0 & -I_3 \end{bmatrix} \quad (34c)$$

$$\begin{bmatrix} \Delta I_1 & \Delta I_2 & \Delta I_3 \end{bmatrix} = \delta_4 \begin{bmatrix} I_1 & -I_2 & 0 \end{bmatrix} \quad (34d)$$

$$\begin{bmatrix} \Delta I_1 & \Delta I_2 & \Delta I_3 \end{bmatrix} = \delta_5 \begin{bmatrix} I_1 & I_2 & -I_3 \end{bmatrix} \quad (34e)$$

where  $\delta_i$ 's represent the amounts of directional parameter variations with respect to the nominal inertias  $I_1$ ,  $I_2$ , and  $I_3$ . The directional variation involving  $\delta_i$  is called a  $\delta_i$ -inertia variation in this paper. As discussed in [4], there exist physical bounds for  $\delta_i$ 's due to the inherent physical properties of the gravity-gradient stabilization and the moments of inertia itself. Table 2 summarizes such physical limitations on  $\delta_i$ -inertia variations. As discussed in [3,4], the Phase 1 Space Station becomes unstable for as little as  $-7\%$  variation in  $I_3$  and  $+8\%$  variation in  $I_1$ , because of the inherent physical nature of the problem.

The robust controller synthesis in this paper is primarily concerned with the  $\delta_1$ - and  $\delta_2$ -inertia variations. In particular, the  $\delta_1$ -inertia variation is physically caused by the translational motion of the payload along the pitch axis, as illustrated in Fig. 1.

### Pitch Control

The pitch-axis dynamics with nominal inertias are described as:

$$\frac{d}{dt} \begin{bmatrix} \theta_2 \\ \dot{\theta}_2 \end{bmatrix} = \begin{bmatrix} 0 & 1 \\ -3n^2 k_2 & 0 \end{bmatrix} \begin{bmatrix} \theta_2 \\ \dot{\theta}_2 \end{bmatrix} + \begin{bmatrix} 0 \\ b_2 \end{bmatrix} [-u_2] \quad (35)$$

where the external disturbance is not included since it is accommodated by the disturbance rejection filter.

Since the  $\delta_1$ -inertia variation does not affect the pitch dynamics (i.e.,  $k_2$  and  $b_2$  remain constant), only the  $\delta_2$ -inertia variation, where only  $b_2$  has uncertainty, is considered for the pitch axis.

An input-output decomposition of the perturbed control distribution matrix  $\Delta B_2$  in Eq. (35) is obtained as

$$\Delta B_2 = \begin{bmatrix} 0 \\ \frac{1}{I_2(1+\delta_2)} - \frac{1}{I_2} \end{bmatrix} = -MEN$$

and

$$M = \begin{bmatrix} 0 \\ b_2 \end{bmatrix}, \quad E = \delta_2', \quad N = -1,$$

where  $b_2 = 1/I_2$  for the nominal inertia and  $\delta_2' = 1/(1 + \delta_2) - 1$ .

The fictitious input  $w_p$  and the fictitious output  $z_p$  for the pitch axis with the  $\delta_2$ -inertia variation are then expressed as

$$z_p = N[-u_2] = u_2 \quad (36a)$$

$$w_p = -Ez_p = -\delta_2' z_p \quad (36b)$$

These equations replace the parameter variations in Eq. (35) as follows:

$$\frac{d}{dt} \begin{bmatrix} \theta_2 \\ \dot{\theta}_2 \end{bmatrix} = \begin{bmatrix} 0 & 1 \\ -3n^2 k_2 & 0 \end{bmatrix} \begin{bmatrix} \theta_2 \\ \dot{\theta}_2 \end{bmatrix} + \begin{bmatrix} 0 \\ b_2 \end{bmatrix} [w_p - u_2] \quad (37a)$$

$$z_p = u_2 \quad (37b)$$

$$w_p = -\delta_2' z_p \quad (37c)$$

where  $k_2 = (I_3 - I_1)/I_2$  with the nominal inertias.

The robust control problem for Eqs. (35) now becomes a disturbance attenuation problem for Eqs. (37), to which Theorems 2 and 3 can be applied. Note that  $z_p$  contains only the control input  $u_2$ . This uncertainty in the control loop introduces a necessary tradeoff between stability robustness and performance.

Equations (37) are now augmented by the pitch CMG momentum dynamics described by Eq. (26b) and disturbance rejection filters described by Eqs. (29c) and (29d). The augmented state vector is  $\mathbf{x}_2$  as defined in Eq. (31), and the controlled output  $\mathbf{z}$  is also formed as

$$\mathbf{z} = \begin{bmatrix} \mathbf{x}_2 \\ u_2 \end{bmatrix}$$

With proper selections of the weighting factors, scaling, and orthogonal transformations, as discussed in the appendix, the augmented system equations are transformed to satisfy the assumption (ii) in Theorem 3. The performance specification bound  $\gamma$  is chosen to be 1, and a set of weighting factors used in this paper is summarized in Table 7.

By solving the Riccati equation, Eq. (22), a robust  $H_\infty$  full-state feedback controller for the pitch axis is obtained with a control gain matrix listed in Table 3. The closed-loop eigenvalues of the nominal system with this gain matrix are listed in Table 4. Stability margins of this new robust  $H_\infty$  controller with respect to the inertia variations are compared in Table 5 to those of the previous LQR design in [3]. A significant margin of 70% for the  $\delta_2$ -inertia variation is achieved (compared to the 34% margin of the LQR design). As can be seen in Table 4, however, this new pitch controller has a closed-loop pole at  $-8.29n$  which is relatively large compared to that of the conventional LQR design of Ref. 3. As discussed in [14], an  $H_\infty$  controller often achieves the desired robustness

by having a high bandwidth for a single input system. The pitch axis design here is such a case; but the robust  $H_\infty$  control design for the multi-input case to be discussed in the next section has a remarkable stability robustness margin with nearly the same bandwidth as the conventional LQR design.

### Roll/Yaw Control

Consider the roll/yaw dynamics with nominal parameters described by

$$\begin{bmatrix} \dot{\theta}_1 \\ \dot{\omega}_1 \\ \dot{\theta}_3 \\ \dot{\omega}_3 \end{bmatrix} = \begin{bmatrix} 0 & 1 & n & 0 \\ -3n^2k_1 & 0 & 0 & -nk_1 \\ -n & 0 & 0 & 1 \\ 0 & nk_3 & 0 & 0 \end{bmatrix} \begin{bmatrix} \theta_1 \\ \omega_1 \\ \theta_3 \\ \omega_3 \end{bmatrix} + \begin{bmatrix} 0 & 0 \\ b_1 & 0 \\ 0 & 0 \\ 0 & b_3 \end{bmatrix} \begin{bmatrix} -u_1 \\ -u_3 \end{bmatrix} \quad (38)$$

where the external disturbances are not included. Variations in  $k_1$ ,  $k_3$ ,  $b_1$ , and  $b_3$  caused by perturbations in the moments of inertia are approximated as follows:

$$\begin{aligned} \Delta k_1 &\cong -k_1 \frac{\Delta I_1}{I_1} + \frac{\Delta I_2}{I_1} - \frac{\Delta I_3}{I_1}, \\ \Delta k_3 &\cong -\frac{\Delta I_1}{I_3} + \frac{\Delta I_2}{I_3} - k_3 \frac{\Delta I_3}{I_3}, \\ \Delta b_1 &\cong -b_1 \frac{\Delta I_1}{I_1}, \quad \Delta b_3 \cong -b_3 \frac{\Delta I_3}{I_3}, \end{aligned}$$

where  $k_1 = (I_2 - I_3)/I_1$ ,  $k_3 = (I_2 - I_1)/I_3$ ,  $b_1 = 1/I_1$ , and  $b_3 = 1/I_3$ , for the nominal inertias.

In particular, for the  $\delta_1$ -inertia variation, the above parameter variations become:

$$\begin{aligned} \Delta k_1 &\cong -(k_1 + 1)\delta_1, & \Delta b_1 &\cong -b_1\delta_1, \\ \Delta k_3 &\cong -(k_3 + 1)\frac{I_1}{I_3}\delta_1, & \Delta b_3 &\cong -b_3\frac{I_1}{I_3}\delta_1. \end{aligned}$$

An input-output decomposition of the perturbed system matrix  $\Delta_e$  is then obtained as:

$$\Delta_e = -M E \begin{bmatrix} N_x & N_u \end{bmatrix}$$

or

$$M = \begin{bmatrix} 0 & 0 \\ b_1 & 0 \\ 0 & 0 \\ 0 & b_3 \end{bmatrix}, \quad E = \begin{bmatrix} \delta_1 & 0 \\ 0 & \delta_1 \end{bmatrix},$$

$$N_x = \begin{bmatrix} -3n^2 I_a & 0 & 0 & -n I_a \\ 0 & n \frac{I_1}{I_3} I_b & 0 & 0 \end{bmatrix},$$

$$N_u = \begin{bmatrix} -1 & 0 \\ 0 & -\frac{I_1}{I_3} \end{bmatrix},$$

where  $I_a \triangleq I_2 - I_3 + I_1$  and  $I_b \triangleq I_2 - I_1 + I_3$ .

The fictitious input  $w_p$  and output  $z_p$  for the roll/yaw control design incorporating the  $\delta_1$ -inertia variation are expressed as

$$z_p = N_x x + N_u \begin{bmatrix} -u_1 \\ -u_3 \end{bmatrix} \quad (39a)$$

$$w_p = -E z_p = -\delta_1 z_p \quad (39b)$$

where  $x \triangleq [\theta_1 \ \omega_1 \ \theta_3 \ \omega_3]^T$ . The perturbed system is then expressed by the nominal system and the internal feedback loop as

$$\dot{x} = Ax + B[w_p - u] \quad (40a)$$

$$z_p = N_x x - N_u u \quad (40b)$$

$$w_p = -\delta_1 z_p \quad (40c)$$

where  $u \triangleq [u_1 \ u_3]^T$ ,  $B \triangleq M$  and

$$A \triangleq \begin{bmatrix} 0 & 1 & n & 0 \\ -3n^2 k_1 & 0 & 0 & -n k_1 \\ -n & 0 & 0 & 1 \\ 0 & n k_3 & 0 & 0 \end{bmatrix}.$$

Similarly to the pitch-axis design, the standard state-space representation given by Eq. (1) can be constructed by redefining  $w$  and  $z$ . A roll/yaw gain matrix of the robust  $H_\infty$  controller is listed in Table 3 for the particular weighting factors chosen as in Table 7. The closed-loop eigenvalues of the nominal system with this robust  $H_\infty$  controller are listed in Table 4. Stability margins of this new controller are compared to those of other previous designs in Table 6. Similarly to the pitch control design, the robust  $H_\infty$  controller for the coupled roll/yaw axes has significant improvement in stability

margins over the standard LQR design (e.g., the 73% margin over the 44% margin for the  $\delta_1$ -inertia variation). Contrary to the pitch case with a single control input, however, the robust  $H_\infty$  controller for the roll/yaw axes with two control inputs has a relatively low bandwidth! In fact, the roll/yaw closed-loop poles shown in Table 4 are very comparable to those of LQR designs in [3-5].

## 5. Discussions

Major results and contributions of this paper are summarized in this section. A robust control synthesis technique presented in Section 2, which is primarily based on the results in [10,13] and the state-space formulation of the  $H_\infty$  control theory in [8,9], further exploits the concept of linearized, directional variations of nonlinear, structured uncertain parameters. Applications of this approach to the full-state feedback control design problem of the Space Station with uncertain inertia property have resulted in the following interesting results: (1) For the pitch control with a single input, the stability robustness improvement with respect to the overall inertia increases has been achieved mainly by having a relatively high bandwidth controller and (2) The robust  $H_\infty$  control design for the roll/yaw axis with two control inputs has achieved significant stability robustness over the LQR design, even with relatively low bandwidth. In other words, the concept of linearized directional parameter variation, combined with the standard  $H_\infty$  control theory, has been shown to be a practical way for designing parameter-insensitive controllers.

For roll/yaw control, the  $\delta_1$ -inertia variation was considered in robust  $H_\infty$  control design to accommodate the moments-of-inertia variations caused by the translational motion of a large payload along the pitch axis (see Fig. 1). Since the  $\delta_1$ -inertia variation does not affect the pitch dynamics, the  $\delta_2$ -inertia variation was considered for the pitch control design. It is also emphasized that the closed-loop system with this new robust  $H_\infty$  controller is stable for  $\pm 73\%$   $\delta_1$ -inertia variation and for  $\pm 70\%$   $\delta_2$ -inertia variation, compared to the  $\pm 44\%$   $\delta_1$  and  $\pm 34\%$   $\delta_2$  stability margins of a typical LQR design.

## 6. Conclusions

A robust control synthesis technique for uncertain dynamical systems subject to nonlinear, structured parameter perturbations has been presented, which is based on

the  $H_\infty$  control theory and the internal feedback loop modeling concept. This technique was applied to the multivariable, full-state feedback control design problem of the Space Station, resulting in remarkable stability margins with respect to the moments-of-inertia uncertainty over the conventional linear-quadratic-regulator designs. The linearized, directional parameter variation concept was shown to be a proper way of accommodating the nonlinear, structured parameter variations in the design of a parameter-insensitive controller.

## Appendix

In general, the  $H_\infty$  control theory considers frequency-dependent weighting matrices for the shaping of closed-loop transfer function  $T_{zw}$ . Proper selection of the weighting matrices, however, is not always obvious. One practical way is to use a constant diagonal weighting matrix and a normalized output equation. Proper scaling and orthogonal transformations can be employed to satisfy the assumptions in Theorem 3.

Consider a system given by

$$\begin{aligned}\dot{x} &= Ax + B_1 w + B_2 u \\ z &= \begin{bmatrix} z^{(1)} \\ z^{(2)} \end{bmatrix} = \begin{bmatrix} C_1^{(1)} \\ 0 \end{bmatrix} x + \begin{bmatrix} D_{12}^{(1)} \\ D_{12}^{(2)} \end{bmatrix} u\end{aligned}$$

where  $D_{12}^{(2)}$  is assumed nonsingular.

Define  $r_{z^{(1)}}$ ,  $r_{z^{(2)}}$ , and  $r_w$  be the weighting factors with dimensions of  $p_1$ ,  $m_2$ , and  $m_1$ , respectively. The weighting matrices  $Q$ ,  $R$ , and  $W$  are then defined as:

$$\begin{aligned}Q &= [\text{diag}\{r_{z^{(1)}}\}]^{-1} \\ R &= [\text{diag}\{r_{z^{(2)}}\}]^{-1} \\ W &= [\text{diag}\{r_w\}]^{-1}\end{aligned}$$

Define normalized variables as

$$\begin{aligned}\bar{z}^{(1)} &= Q z^{(1)} \\ \bar{z}^{(2)} &= R z^{(2)} \\ \bar{w} &= W w\end{aligned}$$

A scaling factor  $S$  for  $u$  is also defined as:

$$\bar{u} = Su$$

Substituting the above new variables into the system equation gives

$$\begin{aligned} \dot{x} &= Ax + B_1 W^{-1} \bar{w} + B_2 S^{-1} \bar{u} \\ \begin{bmatrix} Q^{-1} \bar{z}^{(1)} \\ R^{-1} \bar{z}^{(2)} \end{bmatrix} &= \begin{bmatrix} C_1^{(1)} \\ 0 \end{bmatrix} x + \begin{bmatrix} D_{12}^{(1)} \\ D_{12}^{(2)} \end{bmatrix} S^{-1} \bar{u} \end{aligned}$$

The controlled output equation can be rewritten as

$$\begin{bmatrix} \bar{z}^{(1)} \\ \bar{z}^{(2)} \end{bmatrix} = \begin{bmatrix} QC_1^{(1)} \\ 0 \end{bmatrix} x + \begin{bmatrix} QD_{12}^{(1)} \\ RD_{12}^{(2)} \end{bmatrix} S^{-1} \bar{u}$$

with a QR decomposition of the matrix

$$\begin{bmatrix} QD_{12}^{(1)} \\ RD_{12}^{(2)} \end{bmatrix} = P \begin{bmatrix} 0 \\ L \end{bmatrix}$$

where  $P$  is an orthogonal transformation matrix and  $L$  is lower-triangular (or generally nonsingular).

If the control scaling matrix  $S$  can be defined as

$$S = L^{-1}$$

the following system equation then satisfies the assumptions (ii) and (iv) in Theorem 3:

$$\begin{aligned} \dot{x} &= Ax + B_1 W^{-1} \bar{w} + B_2 L \bar{u} \\ P^T \begin{bmatrix} \bar{z}^{(1)} \\ \bar{z}^{(2)} \end{bmatrix} &= P^T \begin{bmatrix} QC_1^{(1)} \\ 0 \end{bmatrix} x + \begin{bmatrix} 0 \\ I \end{bmatrix} \bar{u} \end{aligned}$$

where  $P^T$  does not affect the  $H_\infty$  norm property.

The system matrices are redefined, to be implemented in a computer software (e.g., CTRL-C), as

$$\begin{aligned} B_1 &\leftarrow B_1 W^{-1}, & B_2 &\leftarrow B_2 L, \\ C_1 &\leftarrow P^T \begin{bmatrix} QC_1^{(1)} \\ 0 \end{bmatrix}, & D_{12} &\leftarrow \begin{bmatrix} 0 \\ I \end{bmatrix}. \end{aligned}$$

Finally the actual control gain matrix  $K$  is obtained by re-scaling the normalized gain matrix  $\bar{K}$  as:

$$K = S^{-1} \bar{K}$$

The weighting factors selected for the example design of this paper are listed in Table 7.

### References

- [1] J.A. Yeichner, J.F. Lee, and D. Barrows, "Overview of Space Station Attitude Control System with Active Momentum Management," AAS Paper No. 88-044, 11th Annual AAS Guidance and Control Conference, 1988.
- [2] H.H. Woo, H.D. Morgan, and E.T. Falangas, "Momentum Management and Attitude Control Design for a Space Station," *Journal of Guidance, Control, and Dynamics*, Vol. 11, No. 1, pp. 19-25, Jan.-Feb., 1988.
- [3] B. Wie, K.W. Byun, V.W. Warren, D. Geller, D. Long, and J. Sunkel, "New Approach to Attitude/Momentum Control of the Space Station," *Journal of Guidance, Control, and Dynamics*, Vol. 12, No. 5, pp. 714-722, Sept.-Oct., 1989.
- [4] V.W. Warren, B. Wie, and D. Geller, "Periodic-Disturbance Accommodating Control of the Space Station," *Journal of Guidance, Control, and Dynamics*, Vol. 13, No. 6, 1990, pp. 984-992.
- [5] J.T. Harduvell, "Comparison of Continuous Momentum Control Approaches for the Space Station," Internal Memo A95-J845-JTH-M-8802099, Space Station Division, McDonnell Douglas Astronautics Co., Sept. 26, 1989.
- [6] J. Sunkel and L.S. Shieh, "An Optimal Momentum Management Controller for the Space Station," AIAA Paper No. 89-3474, to appear in the *Journal of Guidance, Control, and Dynamics*.
- [7] B. Wie, A. Hu, and R. Singh, "Multi-Body Interaction Effects on Space Station Attitude Control and Momentum Management," *Journal of Guidance, Control, and Dynamics*, Vol. 13, No. 6, 1990, pp. 993-999.
- [8] J. Doyle, K. Glover, P. Khargonekar, and B. Francis, "State-Space Solutions to Standard  $H_2$  and  $H_\infty$  Control Problems," *IEEE Transactions on Automatic Control*, Vol. 34, No. 8, pp. 831-847, Aug., 1989.
- [9] K. Glover and J. Doyle, "State-Space Formulae for All Stabilizing Controllers that Satisfy an  $H_\infty$ -norm Bound and Relations to Risk Sensitivity," *Systems & Control Letters*, No.11, pp. 167-172, 1988.
- [10] K.W. Byun, *Robust Controller Synthesis for Uncertain Dynamical Systems*, Ph.D. Dissertation, Dept. of Aerospace Engineering and Engineering Mechanics, The University of Texas at Austin, May 1990.

- [11] B.G. Morton and R.M. McAfoos, "A Mu-Test for Robustness Analysis of a Real-Parameter Variation Problem," *Proc. of ACC*, pp. 135-138, June, 1985.
- [12] M. Tahk and J.L. Speyer, "Modeling of Parameter Variations and Asymptotic LQG Synthesis," *IEEE Transactions on Automatic Control*, Vol. AC-32, No. 9, pp. 793-801, Sept., 1987.
- [13] K.W. Byun, B. Wie, and J. Sunkel, "Robust Control Synthesis for Uncertain Dynamical Systems," AIAA Paper No. 89-3516, to appear in the *Journal of Guidance, Control, and Dynamics*.
- [14] A.E. Bryson, Jr. and A. Carrier, "A Comparison of Control Synthesis Using Differential Games (H-infinity) and LQR," AIAA Paper No. 89-3598.
- [15] B.A. Francis, *A Course in  $H_\infty$  Control Theory*, Springer-Verlag Berlin, Heidelberg, 1987.
- [16] E. Wedell, C.-H. Chuang, and B. Wie, "Stability Robustness Margin Computation for Structured Real-Parameter Perturbations," *Journal of Guidance, Control, and Dynamics*, Vol. 14, No. 3, 1991, pp. 607-614.

Table 1: Space Station Parameters

Parameters	Assembly Flight #3	Phase 1
Inertia (slug-ft <sup>2</sup> )		
$I_{11}$	23.22E6	50.28E6
$I_{22}$	1.30E6	10.80E6
$I_{33}$	23.23E6	58.57E6
$I_{12}$	-0.023E6	-0.39E6
$I_{13}$	0.477E6	0.16E6
$I_{23}$	-0.011E6	0.16E6
Aerodynamic torque (ft-lb) for Phase 1		
$w_1$	$1 + \sin(nt) + 0.5 \sin(2nt)$	
$w_2$	$4 + 2 \sin(nt) + 0.5 \sin(2nt)$	
$w_3$	$1 + \sin(nt) + 0.5 \sin(2nt)$	

Table 2: Physical bounds for  $\delta_i$ -inertia variations

Variation Type	Lower Bound	Upper Bound
$\delta_1$	-78.5 % <sup>†</sup>	$\infty$
$\delta_2$	-100.0 % <sup>*</sup>	$\infty$
$\delta_3$	-2.3 % <sup>*</sup>	+7.6 % <sup>†</sup>
$\delta_4$	-64.6 % <sup>†</sup>	+16.4 % <sup>†</sup>
$\delta_5$	-2.1 % <sup>*</sup>	+7.6 % <sup>†</sup>

<sup>†</sup>due to pitch open-loop characteristic.

<sup>‡</sup>due to roll/yaw open-loop characteristic.

<sup>\*</sup>due to triangle inequalities for the moments of inertia.

Table 3: Robust  $H_\infty$  controller gains for the Phase 1 Space Station

Pitch $K_{22}^T$	Roll/Yaw $K^T$		Units
	6.885E+2	2.559E+2	ft-lb/rad
	4.092E+5	1.448E+5	ft-lb-sec/rad
	2.648E-3	1.495E-3	ft-lb/ft-lb-sec
	-5.563E-7	4.948E-7	ft-lb/ft-lb-sec <sup>2</sup>
	-1.147E-10	-4.142E-10	ft-lb-rad <sup>2</sup> /ft-lb-sec <sup>3</sup>
	5.193E-7	2.263E-7	ft-lb-rad <sup>2</sup> /ft-lb-sec <sup>2</sup>
	-9.374E-10	-9.864E-10	ft-lb-rad <sup>2</sup> /ft-lb-sec <sup>3</sup>
	-3.783E-7	-3.204E-7	ft-lb-rad <sup>2</sup> /ft-lb-sec <sup>2</sup>
4.531E+2	1.800E+2	4.115E+2	ft-lb/rad
2.607E+5	8.914E+4	3.719E+5	ft-lb-sec/rad
1.169E-2	5.124E-4	2.015E-3	ft-lb/ft-lb-sec
4.518E-6	-3.149E-7	-1.997E-7	ft-lb/ft-lb-sec <sup>2</sup>
5.673E-5	-1.567E-5	-8.042E-5	ft-lb-rad/sec <sup>2</sup>
3.598E-2	-6.513E-2	-2.127E-3	ft-lb-rad/sec
-1.722E-5	1.892E-4	-2.489E-4	ft-lb-rad/sec <sup>2</sup>
6.626E-2	8.709E-4	2.506E-2	ft-lb-rad/sec

Table 4: Closed-loop eigenvalues of the Phase 1 Space Station with robust  $H_\infty$  controller, in units of orbital rate,  $n = 0.0011$  rad/sec

	Momentum/ Attitude	Disturbance Filter
Pitch	-0.54 ± 0.54j -1.53, -8.29	-0.10 ± 1.05j -0.10 ± 2.03j
Roll/Yaw	-0.20, -0.21 -0.31 ± 0.87j -0.82 ± 0.85j -2.31 ± 0.65j	-0.13 ± 1.01j -0.33 ± 1.18j -0.10 ± 1.99j -0.27 ± 2.06j

Table 5: Pitch-axis stability robustness comparison

%	LQR		Robust $H_\infty$	
	$\underline{\delta}$	$\bar{\delta}$	$\underline{\delta}$	$\bar{\delta}$
$\delta_1$	-99	$\infty$	-99	$\infty$
$\delta_2$	-89	34	-99	70
$\delta_3$	-17	7	-27	7
$\delta_4$	-19	16	-40	16
$\delta_5$	-30	7	-31	7

\* $\underline{\delta}$  and  $\bar{\delta}$  are lower and upper bounds, respectively.

Table 6: Roll/yaw stability robustness comparison

%	LQR		Local <sup>†</sup>		Robust $H_\infty$	
	$\underline{\delta}$	$\bar{\delta}$	$\underline{\delta}$	$\bar{\delta}$	$\underline{\delta}$	$\bar{\delta}$
$\delta_1$	-78	44	-64	29	-78	73
$\delta_2$	-99	43	-67	30	-99	71
$\delta_3$	-61	80	-60	61	-58	77
$\delta_4$	-64	64	-64	35	-64	99
$\delta_5$	-51	68	-48	50	-49	66

<sup>†</sup>local feedback control (decentralized control).

\* $\underline{\delta}$  and  $\bar{\delta}$  are lower and upper bounds, respectively.

Table 7: Weighting factors used in the example design

Weightings	Pitch	Roll	Yaw	Units
$\theta$	1.5	1.7E-3	2.1E-3	rad
$\dot{\theta}/\omega$	3.8E-3	6.1E-7	7.0E-7	rad/sec
$h$	8.7E+3	1.7E+4	3.0E+4	ft-lb-sec
$\int h$	3.7E+4	1.2E+5	1.8E+5	ft-lb-sec <sup>2</sup>
$\alpha$	3.5E+4	1.6E+8*	9.2E+2	sec <sup>2</sup> /rad
$\dot{\alpha}$	2.1	1.7E+5*	8.0E-1	sec/rad
$\beta$	2.5E+4	3.7E+7*	1.5E+3	sec <sup>2</sup> /rad
$\dot{\beta}$	1.0	3.7E+5*	3.5E-1	sec/rad
$u$	2.7E-2	1.0E-1	1.2E-1	ft-lb
$z_p$	2.7E-2	5.0E-2	5.0E-2	ft-lb
$w_p$	1.0E-2	1.0E-2	1.0E-2	ft-lb

\*in units of ft-lb-sec<sup>3</sup>/rad<sup>2</sup>, ft-lb-sec<sup>2</sup>/rad<sup>2</sup>, ft-lb-sec<sup>3</sup>/rad<sup>2</sup>, and ft-lb-sec<sup>2</sup>/rad<sup>2</sup>, respectively.